chemosensors

MDPI

Article

Silicon MEMS Thermocatalytic Gas Sensor in Miniature Surface Mounted Device Form

Nikolay Samotaev [1,*], Pavel Dzhumaev [1], Konstantin Oblov [1], Alexander Pisliakov [1], Ivan Obraztsov [1], Csaba Ducso [2] and Ferenc Biro [2]

[1] MEPhI (Moscow Engineering Physics Institute), National Research Nuclear University, Kashirskoe Highway 31, 115409 Moscow, Russia; psdzhumaev@mephi.ru (P.D.); kyoblov@mephi.ru (K.O.); palexv_07@mail.ru (A.P.); yuganinn@yandex.ru (I.O.)

[2] Centre for Energy Research, Konkoly-Thege Miklós út 29-33, H-1121 Budapest, Hungary; ducso.csaba@ek-cer.hu (C.D.); biro.ferenc@energia.mta.hu (F.B.)

* Correspondence: nnsamotaev@mephi.ru

Abstract: A reduced size thermocatalytic gas sensor was developed for the detection of methane over the 20% of the explosive concentration. The sensor chip is formed from two membranes with a 150 μm diameter heated area in their centers and covered with highly dispersed nano-sized catalyst and inert reference, respectively. The power dissipation of the chip is well below 70 mW at the 530 °C maximum operation temperature. The chip is mounted in a novel surface mounted metal-ceramic sensor package in the form-factor of SOT-89. The sensitivity of the device is 10 mV/v%, whereas the response and recovery times without the additional carbon filter over the chip are <500 ms and <2 s, respectively. The tests have shown the reliability of the new design concerning the hotplate stability and massive encapsulation, but the high degradation rate of the catalyst coupled with its modest chemical power limits the use of the sensor only in pulsed mode of operation. The optimized pulsed mode reduces the average power consumption below 2 mW.

Keywords: surface mounted device; silicon MEMS; ceramic MEMS; gas sensor; flip-chip

Citation: Samotaev, N.; Dzhumaev, P.; Oblov, K.; Pisliakov, A.; Obraztsov, I.; Ducso, C.; Biro, F. Silicon MEMS Thermocatalytic Gas Sensor in Miniature Surface Mounted Device Form. *Chemosensors* **2021**, *9*, 340. https://doi.org/10.3390/chemosensors9120340

Academic Editor: Simonetta Capone

Received: 25 October 2021
Accepted: 1 December 2021
Published: 3 December 2021

1. Introduction

Combustible gases are among the most serious sources of man-made disasters in the world nowadays, which may result in severe human losses and damage in the built environment. The earth gas related risks will be with us until the decarburizations of energy consumption is completed on a global scale. Therefore, we have to keep on monitoring leaks of combustible gases to prevent the accidents associated with gas explosion. In terms of detection requirements, one must distinguish the ppm level trace detection related to the environmental issues from the alarming case of the explosion risk, which is typically in the range of v%. Nowadays, four gas sensing technologies are commonly used for detecting combustible gases in the environment near the lower explosive limit (LEL): optical, semiconductor, electrochemical, and thermocatalytic. Optical sensors detect variation in light absorption at certain wavelengths specific for each flammable gas (except for H_2, which has no absorption band) [1,2]; the operation principle of semiconductor sensors is based on the change in conductivity of a semiconductor layer when the gas is adsorbed [3–5]; the electrochemical flammable gas sensor measures the current based on the electrochemical reaction on the working electrode inside the solid or liquid electrolytic cell (mainly used for H_2) [6,7]; the thermocatalytic sensor principle is based on a change of the microhotplate temperature when the gas burns on its surface [8,9]. At high concentrations of methane and hydrogen, the thermal conductivity measurement principle can also be used by detecting the temperature loss of the hotplate [10]. The characteristic features of the devices operating with the above principles are well listed and compared in [11]. The oldest but still leading technique in monitoring the combustible gas leaks is the thermocatalytic gas sensor due

to its attractive features, such as performance, costs, durability, and size. Although the selectivity is poor, in many applications the nature of the combustion gas is known, so the sensor can work at the optimum temperature required for the controlled catalysis of the target gas. A measurement algorithm and an empirical equation for calculating the concentration of unknown combustible gas in % of LEL, indicating how explosive the concentration of combustible gas is, have been proposed [12]. However, by applying a multistage heating profile and quick sequential read-out or a multisensor configuration, the nature of the combustible gas and its concentration in the gas mixture can be measured correctly and separately if the nature of the possible flammable gases is known [13,14].

The thermocatalytic sensor is still preferred in alarm systems for measuring combustible gases below LEL concentrations in coal mines, around land pipelines and in the oil refinery industry. Modern research is focusing on the miniaturization of the sensors [14,15], reducing the energy consumption [16] and increasing the stability of the catalysts to provide stable sensitivity in long term [17]. As the thermocatalytic sensor technology has been used in its current form since the beginning of the 1950s [18], they are now going to be outdated in view of their energy consumption and the related encapsulation requirements as well as the latest technology improvements. The small size and the consequent minimized power consumption of the sensor are essential for wearable alarming devices, especially when the sensor is operated in a harsh, explosive environment. Currently, the power consumption of the best bead type thermocatalytic sensor is at least 140 mW for the two sensors, using 10 μ Pt wires covered by 2 μ SiO_2 glass [19], but the typical bead type of the sensors on the market are made from non-covered 20 μ Pt wire [20] and have 190 mW power consumption at 450 °C constant working temperature. Three ways are seen to reduce the power consumption: improving the technology of the microhotplate platforms to get a uniform temperature profile at the lowest temperature needed for the catalysis and achieve it by minimum power dissipation [21–24], increasing the catalyst activity and stability of the gas sensing material [15,18], or by using non stationary methods for measuring flammable gas concentrations in pulsed temperature mode [21,25]. The present work describes the progress in these fields, aiming at the development of a battery-operated wearable methane sensor by introducing a reduced power dissipation hotplate and an SMD compatible ceramic encapsulation technique.

2. Materials and Methods

The developed thermocatalytic device has a pair of full membranes, which are produced by Silicon MEMS technology with two built-in embedded meander-like filaments (microhotplates). The two microhotplates are covered with a layer of catalyst material (which contains metals of platinum group, i.e., Pt and Pd dispersed on Al_2O_3 carrier particles) for the active gas sensitive element and with an inert layer (pure Al_2O_3) for the reference, respectively. The meanders have a double function: they are used as microhotplates to provide the temperature of the chemistry oxidizing reaction but also as resistance thermometers indicators. The microhotplate working temperature is set in the 450–500 °C range, but during operation the exothermic chemical reaction causes a further increase of temperature. This can be detected by the growing resistance of the meander. The reference, i.e., the chemically passive element, is required for the elimination of the effect of other environmental parameters, such as variation of the ambient temperature or variation of other non-combustive components in air (such as humidity content). These phenomena cause thermal conductivity change of the ambient temperature, and affect the meander temperature, thereby leading to a false signal if it were to not be compensated. The reference element has similar thermal characteristics with the active element, but since this does not contain a catalyst, it does not oxidize combustible gases. This element pair is incorporated in a Wheatstone bridge electronic circuit, which is balanced in a neutral environment. In the presence of combustive gases, the increasing temperature on the active element leads to difference in the resistances of the two hotplates, which can be detected by the generated bridge voltage. Usually these elements have different colors: the catalytic layer is dark,

whereas the reference layer is white. Consequently, their different emissivity is visible on graphs exhibiting different slopes of the resistance lines when registered in neutral ambient. Fortunately, this mismatch becomes significant only at very high temperatures, where the thermal loss by the emission becomes comparable to other phenomena.

We designed and manufactured 300 × 500 μm^2 full membrane type microhotplates with 150 μm diameter identical Pt heaters in their centers as a MEMS silicon chip to satisfy the above power dissipation and temperature uniformity requirements. In order to verify the achieved results of the planar sensors and further characterize the catalyst, a conventional "bulk" wire bead type thermocatalytic sensor was also fabricated (the same type as widely present on the market [19] and used in research purposes [13–15]). In the following section we describe the important components from which the sensor was made.

2.1. Silicon MEMS Microhotplate Platform

The SEM image of the silicon MEMS chip with two microhotplate platforms used in this work is presented in Figure 1a. The hot spot diameter on the membrane is 150 μm. The Pt filaments are completely sandwiched between TiO_2/SiO_2 layers, thereby the encapsulated Pt is not directly exposed to air during testing. The applied 25 nm thick TiO_2 layers at both sides of the 350 nm thick Pt filament are used to enhance adhesion to the SiO_2 layers and also to prevent the formation of platinum-titan intermetallic phase during the high temperature operation, i.e., it improves the structural stability and the temperature-resistance characteristics of the Pt heater [26]. KOH etching from the back side of the substrate was used for the membrane release. The microhotplate geometry is also crucial in the sensor response and long-term stability. Moreover, its surface temperature must be uniform in order to minimize the temperature gradient related deterioration phenomena, primarily the electromigration in the filament [27]. In addition, the uniform surface temperature of the microhotplate offers much better selectivity among the target gases with different chemical composition, because of their different activation energies of oxidation. Therefore, the Pt metallization, the geometry, and the structural composition of the microhotplate was designed accordingly to get a decent temperature uniformity as was confirmed by visible pyrometry taken on non-covered microhotplates [23,27]. The heated area has less than ±10 °C temperature difference. The unique design [28] and the technology will be published in a separate paper. The 500 °C hotplate temperature is reached by 28 mW at 1.55 V.

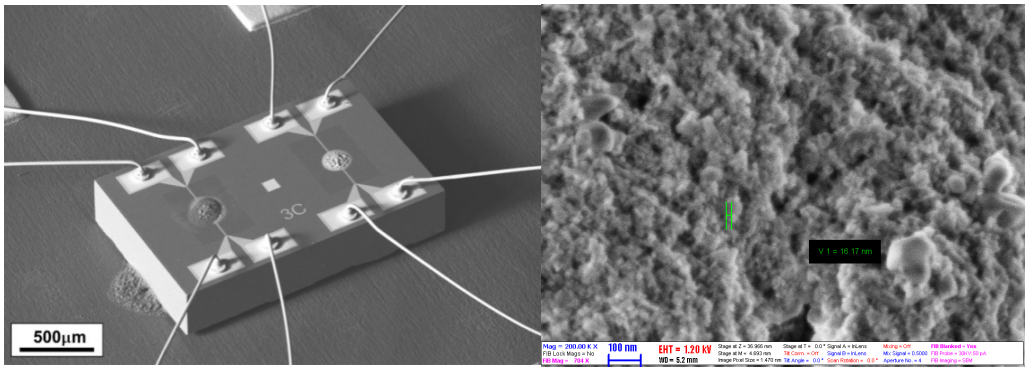

(**a**) (**b**)

Figure 1. Thermocatalytic sensor element: (**a**) SEM image of silicon MEMS chip size is 2 × 1.2 mm^2: The two identical membrane type microhotplates are covered manually with active (dark color) and reference (light color) gas sensitive substances; (**b**) SEM image of active catalytic Al_2O_3 layer deposited on the microhotplate.

Next the wafer was cut to separate chips and drop-coating of inks containing Al_2O_3 particles with and without catalyst were deposited on the microhotplate pairs. Due to the better wettability of the ink of the active material (Al_2O_3 carrier covered by Pt and Pt clusters), the deposited masses of the catalyst and the passive reference material (pure

Al_2O_3 carrier) are different, however, their inks have similar viscosity. This effect produces a thermal mass difference between the passive and the active sensing elements, leading to an initial baseline shift and drift of the response signal during the long-term operation. However, the non-controlled amount of the ink applied manually on different elements may lead to different responses of each device, and in worst case may even modify the temperature-power characteristics. Automation of printing will certainly eliminate this problem. Considering that 0.5 mL minimum volume of ink is needed to measure and confirm the consistency of ink viscosity by using an electronic version brookfield viscometer, this volume is enough to produce a thousand sensors. The chemical power of the catalyst (the generated heat during operation) should surpass the effect of the above mentioned differences, otherwise the sensor response becomes unreliable. Finally, the ink was fired to make the MEMS silicon chip ready for mounting into the ceramic package.

Having a well-controlled catalyst deposition, a power consumption of 28 mW per one microhotplate element is enough to reach the targeted 500 °C operation temperature, however, mismatches in the deposition may increase it with a few mWs. The long time performance of the microhotplates has been tested during experiments. The resistance change of each microhotplate is only about 1.1–1.2% after 6 months of continuous operation at 530 °C. We may conclude that the resistance drift in a Wheatstone-bridge configuration is much less than the required 1% per year for the typical bead-type wire heaters.

2.2. Technology for Catalytic Layer Fabrication

The drop coating technique we used for the catalytic layer deposition determines the viscosity parameters of the applied ink. Handling the viscosity of the ink is crucial for a reliable process; it must be in a range of 50–500 mPa*s, and, as the viscosity also depends on a volume of solid fraction in the ink, the diameter of the solid particles may not exceed 100 nm. The percentage of the solid fraction in the ink may vary between 2030 wt% but it also affects the ink viscosity. The ink viscosity increases exponentially with the addition of a more solid fraction, therefore, the solvent must be added carefully by continuously controlling the viscosity. To fulfill all the requirements, we have chosen pure Al_2O_3 as a catalytic carrier with a characteristic particle size of 60 nm [29]. Before the first operation we divided the material into two equal parts: one of them will be used as the catalyst, whereas the other remains chemically inert and will be used as a reference material; both have similar specific surfaces. We used platinum hexachloro-acid ($H_2PtCl_6{\cdot}6H2O$) [30] and salts of palladium chloride ($PdCl_2$) [31] to obtain noble metal clusters in the catalyst carrier when we annealed it at 500 °C. The next step was the separate mixing of both the active materials and the reference materials with terpineol based solvent to produce appropriate consistence of the inks for deposition onto the MEMS microhotplates by the drop coating technique. The fine tuning of the viscosity discussed above was carried out by carefully evaporating the liquid phase of the ink with active catalytic material. The visible final result of viscosity tuning is the similar patterns of the active and the comparative materials on the microhotplates. The SEM image of the deposited and fired catalysts layer is presented in Figure 1b.

2.3. MEMS Silicon Chip Packaging

In order to miniaturize the device, the sensor chip was encapsulated in a metal-ceramic package in the form of SMD components. The package was designed in the same size as the SOT-89 (4.6 × 4.1 × 1.0 mm). The 3D model of the package, as well as its dimensions in comparison with the metal-glass TO-8 package, are shown in Figure 2b. The SMD sensor package was made of already sintered monolithic ceramic material (96% Al_2O_3) by using the laser micro-milling technique as described in work [32]. The metallization of the ceramic package is based on pure Ag inkjet ink, deposited locally by printing on the selected parts of the ceramic package.

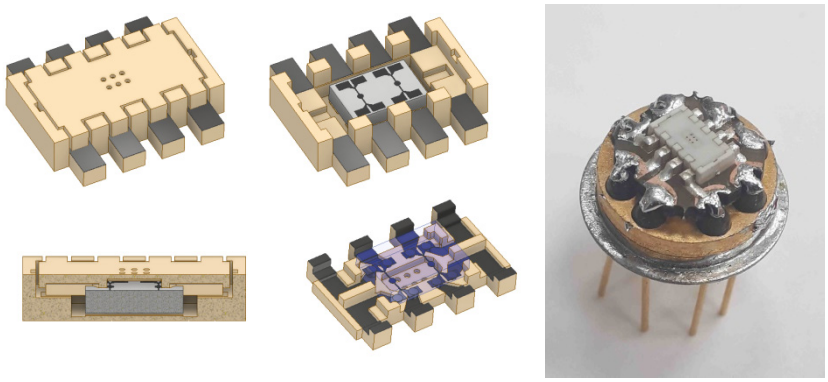

(**a**) (**b**)

Figure 2. SMDsensor package: (**a**) 3D model of the sensor package: dark color—Ag metallization, olive color—Al_2O_3 ceramic, grey color—MEMS silicon chip; (**b**) Self-developed sensor package in SOT-89 form-factor size soldered on PCB mounted in the metal-glass TO-8 package (diameter of top part is ~11 mm [24]).

In the sensor package design, the following factors were taken into account:

- To reduce the process complexity when mounting the MEMS silicon chip in the package (need a cavity under the microhotplate membrane for air pressure compensation);
- To eliminate the Au micro wire bonding/welding operation (as shown in Figure 1) and use the SMD technique for contacting the chip, thereby;
- To decrease the internal space of the package, which would be necessary for the loop of the Au micro wire inside the package;
- To increase the accuracy of the MEMS silicon chip positioning in the package due to the platinum contact pads located on the non-transparent silicone frame of the MEMS silicon chip (the classical task of precisely matching two opaque objects).

Standard flip-chip technology was proposed for mounting the MEMS silicon chip in order to meet the above requirements. The flip-chip technology was modified by considering that the MEMS silicon chip with the micro-heater cannot be mounted upside-down, since the active catalyst needs an air gap on its top to let the ambient diffuse through the holes in the package cap and access the sensing surface. The solution was found in printing the Ag metallization to the inner part of the package cap and gluing the MEMS silicon chip to this metallization using micro dots of Ag paste (image is seen in Figure 3a) directly to platinum contact pads. To position the non-transparent MEMS silicon chip in the package cap correctly, angular guides were micro milled by the laser with an accuracy of 10 μm. This facilitates the accurate positioning of the contact pads on the MEMS silicon chip against the micro Ag glue points (see image in Figure 3b). In order to avoid the short circuiting on the MEMS silicon chip, the Ag dots were deposited in the form of 30 μm columns. After gluing the MEMS silicon chip, an electrical test was carried out (shown in Figure 3c) and the package cap was glued with Ag paste to the basement part of the package. To fix the MEMS silicon chip, drops of the same silver paste, TOK-2 [33], were deposited in the bottom of the package at the corners in order to bond and support the chips on the bottom side as well to eliminate the risk of "hanging the chip from above" in package by the platinum contact pads (which should give weak vibration resistance).

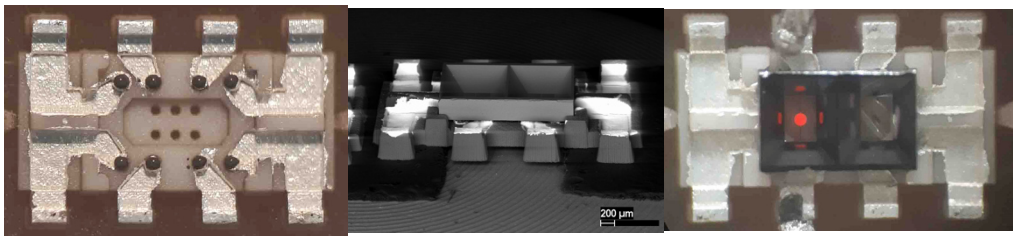

(**a**) (**b**) (**c**)

Figure 3. Mounting silicon MEMS chip into the ceramic package cap with size 3.94 × 2.55 × 0.5 mm: (**a**) Inner part of the sensor package cap before gluing the MEMS silicon chip on micro dot of Ag paste (dark part on metallization); (**b**) SEM photo showing the KOH etched back-side of the glued MEMS silicon chip in the package cap-light color Ag metallization, dark color-Al_2O_3 package cap and MEMS silicon chip; (**c**) the glow at 600 °C working temperature of the Pt microhotplate during the electrical test, which was carried out after gluing the MEMS silicon chip, as seen on the back-side of the chip.

Mounting the MEMS silicon chip in a ceramic package is in principle different from the generally accepted method of gluing the chip to the bottom of the package and welding by Au micro wire, as used by companies to produce microhotplates and MEMS pellistors production, e.g., [34,35]. Our novel approach is very flexible and available for any research teams that need low serial production of semiconductor gas sensor package and perform full-fledged tests in harsh operating conditions, as the ceramics exhibit high resistance to unfavorable environmental factors.

3. Results

At the final stage of the work, series of experiments were carried out to reveal the sensitivity to combustible gases, using methane as a target gas. We are focusing on methane because this is the most critical combustive gas both in terms of its globally widespread application and the known technical challenges when it comes to measuring it. From the total number of the manufactured sensors, three sensors were selected based on imbalance in the readings of the active and comparative elements, which must be minimal. Sensor data are presented in Table 1.

Table 1. Rate of the response signal loss of sensors coated with Pd-Pt catalysts during the stability test.

Sensor Number	Sensitivity Loss (%) [1]	Maximum Response (mV/%vol. CH_4)	Baseline Drift (mV)
1	30	10.5	−1
2	36	10.3	0.7
3	25	11.2	−1

[1] Constant working during four days at 500 °C.

All sensors were connected to the classical Wheatstone bridge electrical circuits used in thermocatalytic gas sensor tests [35]. A PC controlled measuring setup was used for the short- and long-term tests. The minimized volume test chamber was fed by MFC controlled gas lines of N_2, O_2, and CH_4, so as to keep the total flow constant while varying the methane concentrations between 1 and 10 v%. The sensor bridge supply voltage was set to 3.1 V uniformly. The average power consumption of the sensors was 28 mW for one microhotplate (56 mW per one sensor of two microhotplates) at 500 °C. The output voltage of the balanced bridges was measured to four decimals by Keithley 2000 Multimeter. The dependence of the output signal as a voltage difference in the two branches of the Wheatstone bridge electrical circuits vs. methane concentration was registered. For the primary characterization, methane measurements were carried out up to the LEL. The typical sensor response with "fresh" catalyst is presented in Figure 4. This was followed by tests for long-term stability, since it is known that in order to stabilize the properties

of a catalytic material, a few weeks of its annealing in methane containing ambient is required [18].

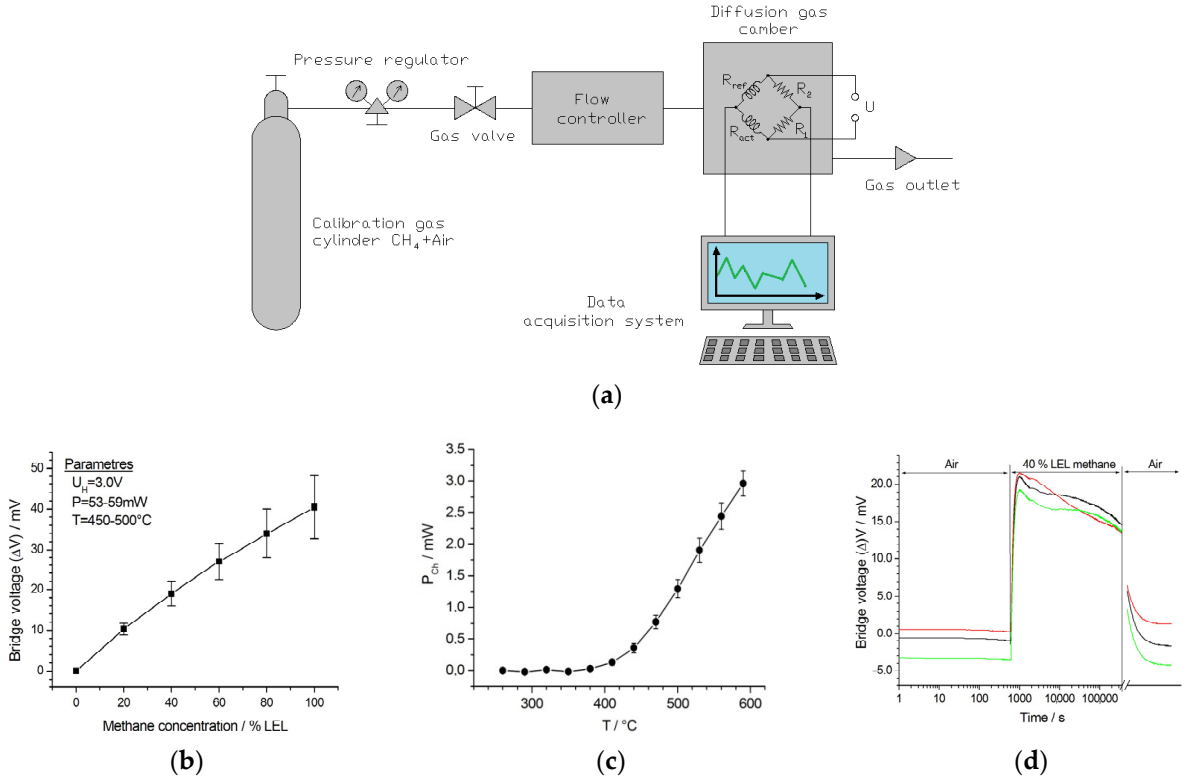

Figure 4. Schematics of the functional test setup. The sensor is inserted in a small volume test chamber fed by mass flow controlled gas composition. The gas flow and its composition as well as the sensor power and read-out are programmable for long testing the long-term performance. The Wheatstone-bridge symbolizes the basic circuit; (**b**) responses to CH_4 in air as the function LEL concentration; (**c**) chemical power (P_{Ch}) measured at 100% LEL methane concentration as a function of working temperature; (**d**) response signal of MEMS thermocatalytic sensor as a function of time during the methane stability test.

During the long-term test, the sensors were exposed to 40% LEL CH_4 in synthetic air and repeated sequentially after every 10 min long synthetic air cycle. The total length of the measurement was four days. The response signal as function of time for different sensors are summarized in Figure 4c. Continuous sensitivity loss can be observed for the three sensors, but the rate of sensitivity loss is same. The percentages of the total sensitivity losses at the end of the test were calculated referring to the maximum response signal. The results are summarized in Table 1.

Although the catalytic activity of the investigated gas sensitive material is not ideal, it enables us to operate the microhotplates around 500 °C, which is definitely better in terms of the long-term stability of the heater and the catalyst as well [12,23]. One of the main parameters of the gas sensing material is the reproducibility of the responses, therefore it was also tested for 250 days at 450 °C constant working temperature in air.

Since the chemical power of the developed catalyst in this volume is not suitable for long-term use of a MEMS sensor, the next long-term tests were performed on a standard bead type sensor with similar parameters of the work [18]. The sensor, in this case, is a hollow cylinder, whose frame is a heating coil made of platinum microwire (diameter of 10 µm) in quartz-shaped insulation (2 µm thick) covered by the developed catalyst (for deposition, the viscosity of the ink containing catalyst increased). The inner and outer diameters of the coil are ~200 µm and ~350 µm, respectively (Figure 5a). The power consumption is 150 mW for the two beads (active and reference) in continuous 450 °C measurement mode. The sensitivity loss of the catalyst is presented in Figure 5b.

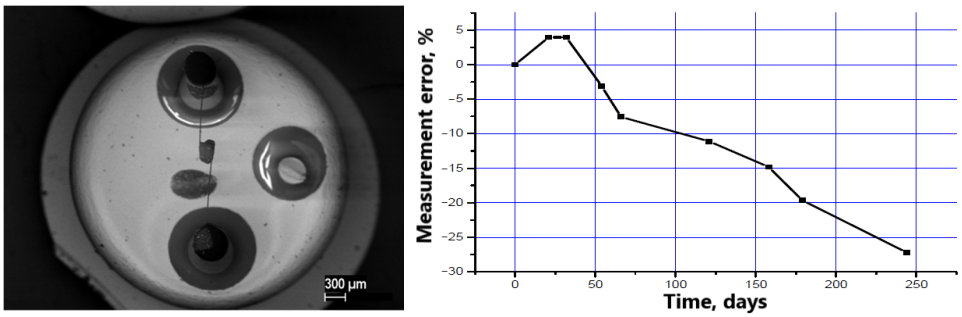

(**a**) (**b**)

Figure 5. The gas sensitivity test of the bead thermocatalytic sensor with constant temperature method: (**a**) SEM image of active bead element cover by the Pt-Pd catalyst (Pt wire welded on TO-18 package holder-diameter of top part is ~4.25 mm); (**b**) the sensitivity losses trend in 2.5 vol.% CH_4 in air for the used catalyst during 250 days (8 months) tests under constant 450 °C working temperature in air (the drop of the initial maximum signal as calculated from the response differences of the active and comparative elements).

If we compare the long-term catalyst activity of the planar MEMS chip and the volumetric bead type sensors (Figures 4 and 5), we can summarize that they are physically the same, but the volumetric sensor has a reserve of catalytic material in the depth of the volume, whereas the planar sensor is deprived of this possibility. We may assume that due to the nano-sized catalytic carrier particles the degradation of the catalytic material in the "bulk" bead type sensor proceeds from the surface to the middle of the bead volume, since the response of the material decreases evenly, without local extremes. At every moment, a small outer diffusion layer is involved in the catalytic oxidation of methane, to a depth of which the gas is able to diffuse until it totally burns at high temperatures; therefore, we expect a longer operation time of the bead type system. Nevertheless, the long-term reliability of the catalyst is still an open and crucial issue; therefore, we focus on the investigation of mixed Pt-Pd and additional components of catalysts to facilitate the selection of the best composition to apply in the MEMS type devices as well.

4. Discussion

The synthesized catalyst is more powerful compared to those we used earlier in our previous works [12]. However, the still existing need to raise the temperature leads to its rapid degradation, especially when it is exposed to combustible gas. The elevated temperature during sensing accelerates the agglomeration of particles of the catalyst carrier and reduces its active surface, and thereby the chemical power. The evident option to improve the lifetime of the device can be the sequential operation in pulsed mode. This operation mode (0.2/4.8 s on/off cycle) is still recommended for the only available MEMS silicon microhotplate catalytic sensor of the SGX company [24] in the market (declaring an average power consumption of 4.8 mW). A similar operation gives an average power consumption of 2.2 mW for our presented MEMS sensor. As the thermo-inertial constant of our sensors are lower compared with the SGX sensor, it is possible to further reduce the lengths of the duty cycle to get an average power consumption of 1.1 mW.

The power can also be reduced by eliminating the reference element from work like it was done in [22]. Nevertheless, the primary reason for using a Wheatstone-bridge circuit is in fact to have measurements that are much less affected by the environmental factors (except the changes in the ambient temperatures that shift the heater temperatures). On the other hand, if the measurements are taken twice per minute, in line with the requirements of the European standards EN 50194:2000 for detection of combustible gases [36], the average power consumption is as low as 45 µW. The proposed method of the sensor operation implies good perspectives for further research. The operation temperature is in fact an additional parameter which can be exploited to extract additional information; e.g., to improve selectivity when a gas mixture is measured. Apart from optimizing voltage pulses

with respect to energy consumption, the device can be combined with thermal conductivity measurement to determine methane concentration well above LEL.

5. Conclusions

A reduced power dissipation MEMS thermocatalytic sensor was developed for combustible gas detection, offering ultralow power consumption in pulsed operation mode. The power dissipation of the chip is below 70 mW at the 530 °C maximum operation temperature. The adaptation of the laser micro milling technology enables the encapsulation of the sensor in miniature SMD SOT-89 fully functional package. The introduction of a modified flip-chip method simplifies the sensor assembly. The novel assembly technique is available for researchers in the field of gas sensors and offers the possibility to test their devices in harsh environment.

The synthesized catalytic material based on an Al_2O_3 carrier coated with clusters of Pt and Pd nanoparticles initially showed a high response. The initial sensitivity of the device is 10 mV/v%, whereas the response and recovery times without the additional carbon filter over the chip are <500 ms and <2 s, respectively. The catalyst still exhibits a rapid degradation for a planar microhotplate design but a slightly better stability for the conventional bulky reference. Therefore, the need for a new catalyst material and its synthesis technique, as well as the further development the measuring technique, are essential to form a long-term reliable MEMS chip based sensor. The recommended option to improve the lifetime of the device can be its operation in pulsed mode with high ratio of the off/on cycle, which still meets the European safety standard.

Author Contributions: Conceptualization, N.S.; methodology, C.D., F.B.; validation, A.P.; investigation, I.O., P.D.; data curation, K.O.; writing—review and editing, N.S.; supervision, N.S.; funding acquisition, N.S., C.D. All authors have read and agreed to the published version of the manuscript.

Funding: This research was supported by the National Research, Development and Innovation Office Foundation of Hungary, Grant No. 2017-2.3.4-TeT-RU-2017-00006, and the Ministry of Science and Higher Education of the Russian Federation founding with unique identifier RFMEFI58718X0053.

Institutional Review Board Statement: Not applicable. No humans or animals were subject of this research.

Informed Consent Statement: Not applicable.

Conflicts of Interest: The authors declare no conflict of interest. The funders had no role in the design of the study; in the collection, analyses, or interpretation of data; in the writing of the manuscript, or in the decision to publish the results.

References

1. Hodgkinson, J.; Tatam, R. Optical gas sensing: A review. *Meas. Sci. Technol.* **2012**, *24*, 012004. [CrossRef]
2. Fanchenko, S.S.; Baranov, A.M.; Savkin, A.V.; Samotaev, N.N. Light emitting diode absorption spectroscopy for combustible gas monitoring. *IOP Conf. Ser. Mater. Sci. Eng.* **2016**, *151*, 012021. [CrossRef]
3. Barsan, N.; Koziej, D.; Weimar, U. Metal oxide-based gas sensor research: How to? *Sens. Actuators B Chem.* **2007**, *121*, 18–35. [CrossRef]
4. Samotaev, N.N.; Podlepetsky, B.I.; Vasiliev, A.A.; Pisliakov, A.V.; Sokolov, A.V. Metal-oxide gas sensor high-selective to ammonia. *Autom. Remote Control* **2013**, *74*, 308–312. [CrossRef]
5. Degler, D.; Müller, S.A.; Doronkin, D.E.; Wang, D.; Grunwaldt, J.-D.; Weimar, U.; Barsan, N. Platinum loaded tin dioxide: A model system for unravelling the interplay between heterogeneous catalysis and gas sensing. *J. Mater. Chem. A* **2018**, *6*, 2034–2046. [CrossRef]
6. ME3-H2 Electrochemical Hydrogen Gas Sensor. Available online: https://www.winsen-sensor.com/sensors/h2-sensor/me3-h2.html (accessed on 1 December 2021).
7. Hydrogen Gas Sensor H2/CT-40000. Available online: https://www.membrapor.ch/sheet/Hydrogen-Gas-Sensor-H2-CT-40000.pdf (accessed on 1 December 2021).
8. Somov, A.; Karelin, A.; Baranov, A.; Mironov, S. Estimation of a Gas Mixture Explosion Risk by Measuring the Oxidation Heat within a Catalytic Sensor. *IEEE Trans. Ind. Electron.* **2017**, *64*, 9691–9698. [CrossRef]
9. Bíró, F.; Dücső, C.; Radnóczi, G.Z.; Baji, Z.; Takács, M.; Bársony, I. ALD nano-catalyst for micro-calorimetric detection of hydrocarbons. *Sens. Actuators B Chem.* **2017**, *247*, 617–625. [CrossRef]

10. MP-7217-TC Combined Flammable and Volume Percent Methane Sensor. Available online: https://www.sgxsensortech.com/content/uploads/2015/01/DS-0152-MP-7217-TC-Datasheet-V2.pdf (accessed on 1 December 2021).
11. Dey, A. Semiconductor metal oxide gas sensors: A review. *Mater. Sci. Eng. B* **2018**, *229*, 206–217. [CrossRef]
12. Karelin, A.; Baranov, A.M.; Akbari, S.; Mironov, S.; Karpova, E. Measurement Algorithm for Determining Unknown Flam-mable Gas Concentration Based on Temperature Sensitivity of Catalytic Sensor. *IEEE Sens. J.* **2019**, *19*, 4173–4180. [CrossRef]
13. Ivanov, I.; Baranov, A.M.; Akbari, S.; Mironov, S.; Karpova, E. Methodology for estimating potential explosion hazard of hydrocarbon with hydrogen mixtures without identifying gas composition. *Sens. Actuators B Chem.* **2019**, *293*, 273–280. [CrossRef]
14. Kulinyi, S.; Brandszajsz, D.; Amine, H.; Adam, M.; Furjes, P.; Barsony, I.; Ducso, C. Olfactory detection of methane, propane, butane and hexane usingconventional transmitter norms. *Sens. Actuators B Chem.* **2005**, *111–112*, 286–292. [CrossRef]
15. Samotaev, N.; Pisliakov, A.; Filipchuk, D.; Etrekova, M.; Biro, F.; Ducso, C.; Bársony, I. SOI Based Micro-Bead Catalytic Gas Sensor. In *International Youth Conference on Electronics, Telecommunications and Information Technologies*; Springer: Cham, Switzerland, 2013; Volume 255, pp. 105–111. [CrossRef]
16. Kalinin, I.; Roslyakov, I.; Tsymbarenko, D.; Bograchev, D.; Krivetskiy, V.; Napolskii, K. Microhotplates based on Pt and Pt-Rh films: The impact of composition, structure, and thermal treatment on functional properties. *Sens. Actuators A Phys.* **2021**, *317*, 112457. [CrossRef]
17. Ivanov, I.I.; Baranov, A.M.; Talipov, V.A.; Mironov, S.M.; Akbari, S.; Kolesnik, I.V.; Orlova, E.D.; Napolskii, K.S. Investigation of catalytic hydrogen sensors with platinum group catalysts. *Sens. Actuators B Chem.* **2021**, *346*, 130515. [CrossRef]
18. Karpova, E.; Mironov, S.; Suchkov, A.; Karelin, A.; Karpov, E.E.; Karpov, E.F. Increase of catalytic sensors stability. *Sens. Actuators B Chem.* **2014**, *197*, 358–363. [CrossRef]
19. Karpov Sensor. Available online: http://karpov-sensor.com/wp-content/uploads/2019/04/DTK1-RV.pdf (accessed on 18 October 2021).
20. Alphasense Inc. Available online: https://www.alphasense.com/wp-content/uploads/2015/04/CHA3.pdf (accessed on 18 October 2021).
21. Vasiliev, A.; Pavelko, R.; Gogish-Klushin, S.Y.; Kharitonov, D.Y.; Gogish-Klushina, O.; Sokolov, A.; Pisliakov, A.; Samotaev, N. Alumina MEMS platform for impulse semiconductor and IR optic gas sensors. *Sens. Actuators B Chem.* **2008**, *132*, 216–223. [CrossRef]
22. Karpov, E.E.; Suchkov, A.; Mironov, S.; Baranov, A.; Sleptsov, V.; Calliari, L. Energy efficient planar catalytic sensor for methane measurement. *Sens. Actuators A Phys.* **2013**, *194*, 176–180. [CrossRef]
23. Biro, F.; Ducso, C.; Hajnal, Z.; Pap, A.E.; Barsony, I. Optimisation of Low Dissipation Micro-Hotplates-Thermo-Mechanical Design and Characterization. In Proceedings of the THERMINIC 2013 19th International Workshop on Thermal Investigations of ICs and Systems, Berlin, Germany, 25–27 September 2013; pp. 116–121. [CrossRef]
24. SGX Sensortech. Available online: https://www.sgxsensortech.com/content/uploads/2014/08/Pulsed-Power-Operation-of-the-MPEL-MEMS-Pellistor.pdf (accessed on 18 October 2021).
25. Somov, A.; Baranov, A.; Suchkov, A.; Karelin, A.; Mironov, S.; Karpova, E. Improving interoperability of catalytic sensors. *Sens. Actuators B Chem.* **2015**, *221*, 1156–1161. [CrossRef]
26. Biro, F.; Hajnal, Z.; Dücső, C.; Barsony, I. The Role of Phase Changes in TiO_2/Pt/TiO_2 Filaments. *J. Electron. Mater.* **2018**, *47*, 2322–2329. [CrossRef]
27. Bíró, F.; Hajnal, Z.; Dücső, C.; Bársony, I. The critical impact of temperature gradients on Pt filament failure. *Microelectron. Reliab.* **2017**, *78*, 118–125. [CrossRef]
28. HU 5279, U2000150. Available online: http://epub.hpo.hu/e-kutatas/?lang=EN (accessed on 1 December 2021).
29. Merck KGaA. Available online: https://www.sigmaaldrich.com/RU/en/product/aldrich/642991?context=product (accessed on 1 December 2021).
30. Merck KGaA. Available online: https://www.sigmaaldrich.com/RU/en/product/sigald/206083?context=product (accessed on 1 December 2021).
31. Merck KGaA. Available online: https://www.sigmaaldrich.com/RU/en/product/aldrich/520659?context=product (accessed on 1 December 2021).
32. Samotaev, N.N.; Oblov, K.Y.; Gorshkova, A.V.; Ivanova, A.V.; Philipchuk, D.V. Ceramic packages prototyping for electronic components by using laser micromillingtechnology. *J. Phys. Conf. Ser.* **2020**, *1686*, 012010. [CrossRef]
33. JSC NIIEM. Available online: https://nii-em.ru/catalog/klei-epoksidnye-tokoprovodyashie (accessed on 18 October 2021).
34. Figaro Engineering Inc. Available online: https://www.figaro.co.jp/en/product/feature/tgs8100.html (accessed on 18 October 2021).
35. Abhishek, K.; Kingson, T.M.G.; Verma, R.P.; Mandal Dutta, R.S.; Chaulya, S.K.; Prasad, G.M. Application of Gas Monitoring Sensors in Underground Coal Mines and Hazardous Areas. *Int. J. Comput. Technol. Electron. Eng.* **2013**, *3*, 9–23.
36. Standard EN 50194:2000, Electrical Apparatus for the Detection of Combustible Gases in Domestic Premises, Test Methods and Performance Requirements. 2000. Available online: https://standards.iteh.ai/catalog/standards/clc/8c7ddffe-5360-45d8-9090-8423c13e702e/en-50194-2000 (accessed on 1 December 2021).